Published in final edited form as:
Exp Cell Res. 2010 July 15; 316(12): 1958–1965. doi:10.1016/j.yexcr.2010.03.018.

Nonmuscle Myosin IIB, a sarcomeric component in the Extraocular Muscles

Carole L. Moncman[1,*] and **Francisco H. Andrade**[2]

[1]Department of Molecular and Cellular Biochemistry, University of Kentucky, 741 S. Limestone, Lexington, KY 40536

[2]Department of Physiology, University of Kentucky, 741 S. Limestone, Lexington, KY 40536

Abstract

Extraocular muscles (EOMs) are categorized as skeletal muscles; however, emerging evidence indicates that their gene expression profile, metabolic characteristics and functional properties are significantly different from the prototypical members of this muscle class. Gene expression profiling of developing and adult EOM suggest that many myofilament and cytoskeletal proteins have unique expression patterns in EOMs, including the maintained expression of embryonic and fetal isoforms of myosin heavy chains (MyHC), the presence of a unique EOM specific MyHC and mixtures of both cardiac and skeletal muscle isoforms of thick and thin filament accessory proteins. We demonstrate that nonmuscle myosin IIB (nmMyH IIB) is a sarcomeric component in ~20% of the global layer fibers in adult rat EOMs. Comparisons of the myofibrillar distribution of nmMyHC IIB with sarcomeric MyHCs indicate that nmMyH IIB co-exists with slow MyHC isoforms. In longitudinal sections of adult rat EOM, nmMyHC IIB appears to be restricted to the A-bands. Although nmMyHC IIB has been previously identified as a component of skeletal and cardiac sarcomeres at the level of the Z-line, the novel distribution of this protein within the A band in EOMs is further evidence of both the EOMs complexity and unconventional phenotype.

Keywords

cytoskeleton; thick filament; tonic fibers

Introduction

The extraocular muscles (EOMs) are responsible for voluntary and reflexive eye movements as the final effectors of the ocular motor system; these small muscles are continuously active during awake periods and regularly during sleep (REM phase). Based on origin, morphology and function, EOMs belong to a very specialized subset of the skeletal muscle class. Unlike the somite-derived skeletal muscles, EOMs originate from mesodermal primordia associated with the neural crest and follow a different developmental program, at least initially [1-3]. Ontological differences correlate then with phenotypical divergence in the adult EOMs, which include the expression of fetal, neonatal and adult striated muscle myosin isoforms throughout

*Corresponding author: Phone number: 859-257-6776, Fax number: 859-323-1037, cmonc2@uky.edu

adulthood, including a unique tissue-specific myosin, Myh13 or EOM-specific myosin [4-6]. Somitic skeletal muscles shut down the expression of both the embryonic and fetal MyHC isoforms soon after birth; these isoforms do not reappear in the adult except during bouts of regeneration [7]. The transition to the adult complement of myosin isoforms in adult EOMs also takes place after birth but the process is influenced by visual experience. For example, the expression of Myh13 and slow myosin isoforms decreases significantly in rodents reared in total darkness from birth; this leads to changes in functional properties as well [5,8].

The sarcomeric differences in the EOMs extend to other structural proteins as well. Rodent EOM fibers do not have M-lines in the A-band, and contain very low mRNA levels of the M-line proteins, myomesin and M-protein [8-11]. Instead, the myomesin isoform expressed in EOMs is EH-myomesin, a splice variant originally identified in embryonic heart and not present in other adult skeletal muscles [8,12,13]. Another member of the M-line, muscle-specific creatine kinase (CK-M), is also reduced in the EOMs [8]. Moreover, gene profiling studies demonstrated the presence of a number of cardiac myofibrillar transcripts: cardiac-specific isoforms of actin, troponin, tropomyosin and nebulette [11,14,15]. Recently, proteomic analysis of rodent EOMs confirmed the presence of α-cardiac actin [16]. We analyzed the nebulin isoforms present in EOMs and found that nebulin, not the cardiac-specific nebulette, is the major nebulin family member expressed [17]. The immunological detection of nebulin in EOMs does not, however, preclude the possibility that nebulette or its splice variant LIM-nebulette [18] is present in low abundance or within specialized domains in EOM fibers.

Recently, we began a systematic survey of the expression pattern of myofibrillar and cytoskeletal proteins in rodent EOMs. One striking result was the presence of nonmuscle myosin IIB (nmMyH IIB, Myh10) in ~20% of global layer fibers in the adult rat EOM. Further analysis of the distribution of nmMyH IIB demonstrates that this myosin is in the sarcomeric A-band of slow tonic EOM fibers, suggesting a role for nmMyH IIB in tonic contraction of these muscles.

Materials and methods

Animals and tissue collection

The Institutional Animal Care and Use Committee at the University of Kentucky approved this study. Adult Sprague Dawley rats (300-350 grams) and C57BL/6 mice (8 weeks old) were euthanized by CO_2 asphyxia followed by pneumothorax. Whole orbits, whole EOM, and gastrocnemius muscle bundles were collected and placed either in 2 M sucrose, 10 mM EDTA, PBS [19] or relaxing solution (100 mM KCl, 20 mM Imidazole, 2 mM EGTA, 4 mM ATP, 7 mM $MgCl_2$). Samples collected for longitudinal sections were pinned in place on corkboard and stretched in the presence of relaxing buffer. All tissues were embedded in OTC and flash frozen in 2-methylbutane cooled to its freezing point in liquid nitrogen.

Immunofluorescence confocal microscopy

Cryostat sections for both cross and longitudinal sections were cut in 10 μm sections using a MICROM HM525 cryostat and collected on superfrost plus slides. Antibodies for nmMyH IIB were purchased from Sigma (St. Louis, MO), Covance (Trenton, NJ) and the Developmental Studies Hybridoma Bank (DSHB, University of Iowa). Myosin antibodies were also from DSHB: embryonic (F1.652), neonatal slow/fast 2A (N2.261), adult slow (A4.951), adult 2A (2F7), adult 2B (10F5), adult 2X (6H1) and all fast isoforms (MF20 and F59). Anti-α-actinin antibody and rhodamine-phalloidin were purchased from Sigma (St. Louis, MO). Immunolabeling was performed as described previously [20]. Briefly, cryostat sections were treated with 1% Triton X-100 in phosphate buffered saline (PBS) for 15 min. at 4°C, washed

and then blocked in 1% normal goat serum in PBS for 1-2 hrs at 4°C. Primary antibodies were diluted in the blocking solution and all incubations were performed at 4°C. Following washes after the primary antibody, secondary antibodies diluted in blocking solution were applied. Secondary antibodies were purchased from Jackson ImmunoResearch and all were minimal cross-reacting antibodies, absorbed against both mouse and rat serum proteins. After washing the samples, either Vectashield (Vector Labs) or ProLong Gold (Molecular Probes) was used to mount the cover slips. Samples were visualized on an Axiovert 200M equipped with an Orca ER camera or on a Leica SP5 confocal.

Data analysis

Fibers were scored as positive when containing nmMyH IIB or negative when not. The percent of positive fibers was calculated as the positives divided by the total number of fibers in the field. Distance measurements and labeling widths were performed on calibrated confocal micrographs using Image J (Rasband, W.S. National Institutes of Health, http://rsb.info.nih.gov/ij/). All statistical analyses were performed using KaleidaGraph. All statistical analyses are reported as the mean±the standard error of the mean. For all measurements, at least 2 animals were used for these observations.

Results

The main EOMs (4 rectus and 2 oblique muscles) have their fibers arranged in two layers, one close to the eye itself (global layer, larger fibers) and one facing the bony orbit (orbital layer, smaller fibers), as can be appreciated in figure 1A. This layer distribution is one of the factors considered for EOM fiber type classification; the other two being mitochondrial content and innervation (single *vs.* multiple innervation) [21]. We used antibodies against the nmMyH IIB and IIA during our initial characterization of the distribution of cytoskeletal proteins within all orbital structures in rodent eyes. Unexpectedly, we observed that a set of fibers within the global layers exhibited intense labeling with a polyclonal antibody raised against the non-helical tailpiece of nmMyH IIB (Fig. 1B, note arrows). To confirm this distribution, rat EOMs were stained with another polyclonal antibody raised against the same epitope (Covance) and a monoclonal antibody to nmMyH IIB (CMII 23). We observed similar distributions of nmMyH IIB positive fibers with the three antibodies (Fig. 2A-C, note arrows). In contrast, nmMyH IIA was observed only in the vasculature and nonmuscle cells, but not within EOM fibers (Fig. 2D, note arrowheads). We scored EOM fibers as positive or negative for a strong cytoplasmic staining for nmMyH IIB in sections from 3 rats and found that they represent 19.56 ±0.95% of the fibers in the global layer. We did not detect nmMyH IIB positive fibers in the orbital layers or in retractor bulbi, an accessory muscle that surrounds the optic nerve.

Our next step was to determine which EOM fiber types are nmMyH IIB positive. We labeled EOM cross-sections with sarcomeric MyHC isoform-specific and nmMyH IIB antibodies. All EOM nmMyH IIB positive fibers also had slow myosin isoforms (Fig. 3A, B). We did not find nmMyH IIB positive fibers that co-expressed any of the fast myosin isoforms (fast 2A is shown in Fig. 3C). Consistent with this result, N2.261 exhibits cross reactivity with adult MyHC fast 2A and we detect additional fibers with this antibody that are negative for nmMyH IIB (Fig. 3B).

Takeda et al. [22] demonstrated that nmMyH IIB could be found in the Z-lines of human cardiac and skeletal muscles. We first studied longitudinal sections from freshly excised flash-frozen EOMs and gastrocnemius muscle bundles (a hind limb muscle) to characterize the sarcomeric distribution of nmMyH IIB. In nmMyH IIB positive EOM fibers, nmMyH IIB was consistently found midway between the α-actinin labels that marked the Z-line (note arrows in Fig. 4A). In these sections, the frequency of nmMyH IIB distribution was 2.0 μm. We were unable to detect nmMyH IIB in gastrocnemius using the same conditions as for EOMs (Fig. 4B). When we

increased the primary antibody concentration and used the gastrocnemius to set the gain and offset for the confocal microscope, we could detect a weak Z-line signal for nmMyH IIB in both the EOM and gastrocnemius, but then the nmMyH IIB positive EOM fibers were so saturated that their sarcomeric distribution was not discernable (not shown).

To demonstrate that these results were not a consequence of muscle contractures prior to freezing, we treated rat EOMs with relaxing buffer in the presence of Triton X-100 in order to remove the sarcolemma (skinned fibers). We then stretched the muscles slightly prior to freezing and sectioning. These samples were labeled for the distribution of actin, α-actinin and nmMyH IIB and examined by confocal microscopy (Fig. 5). nmMyH IIB-positive fibers clearly show this protein within the A-band with a banding pattern of 2.5-2.8 μm midway between the actin/α-actinin labels of the sarcomere (note arrows in Fig. 5A). In some EOM fibers, we also detected nmMyH IIB in the Z-line by increasing the gain on the confocal microscope (note arrowheads in Fig. 5B). Under these conditions, the nmMyH IIB-positive fibers could still be observed with a distinct A-band distribution, but the signal was broadly spread (note arrows in Fig. 5B). To confirm the A-band localization of nmMyH IIB in slow myosin-containing EOM fibers, we imaged relaxed longitudinal sections of rat EOMs labeled with antibodies to slow sarcomeric myosin and nmMyH IIB. The anti-nmMyH IIB antibody decorated a strip in the center of the A-band (Fig. 6A, arrows mark the position of the nmMyH IIB in each field). Finally, the A-band distribution of nmMyH IIB in longitudinal EOM sections was not affected by paraformaldehyde fixation (Fig. 6B, arrows mark the position of the nmMyH IIB in each field).

To address whether the A-band distribution of nmMyH IIB was exclusive to rats, we examined mouse EOMs in both cross and longitudinal sections. As with rat EOMs, we observed 18.9 ±0.9% of mouse EOM fibers were nmMyH IIB positive in the global layer (n=2 mice). There were no nmMyH IIB positive fibers in the orbital layer or in retractor bulbi (not shown). In longitudinal mouse EOM sections labeled for nmMyH IIB and α-actinin or slow sarcomeric myosin, nmMyH IIB was found in the middle of the A-band (Fig. 7).

Measurements from high magnification confocal images of the sarcomeric nmMyH IIB distributions indicate a labeling width of 220±5 nm (n=100 bands, 3 rats) with an A-band width of 1.64±0.01 μm in most fibers. Fifteen percent of the fibers examined had nmMyH IIB labeling widths in excess of 300 nm. We are currently evaluating whether this variability is due to the position of the fibers within the muscles. Nevertheless, the sarcomeric distribution of nmMyH IIB in greater than 85% of the EOM fibers examined is consistent with the known width of the bare zone for sarcomeric native thick filaments [23]. The labeled band in mouse EOM fibers averaged 229±5 nm in width (n=88 **bands**, 2 mice). As with the rat, we also observed a number of bands in which the nmMyH IIB labeling was in excess of 300 nm wide, but again over 85% of the measurements are consistent with the width of the bare zone.

Discussion

The results from this study demonstrate that nmMyH IIB is found in the sarcomeric A-band of slow global EOM fibers, yet another novel structural feature of these muscles. While other investigators had shown that nonmuscle and sarcomeric myosins co-polymerize in *in vitro* systems [24,25], the EOMs are the first example of such an arrangement *in vivo*. Since the slow tonic EOM fibers have been postulated to have a role in fixation, the inclusion of nmMyH IIB in these fibers may be important for this function [26,27].

Like sarcomeric myosins, nonmuscle myosins form filaments at physiological ionic strength, but they are only ~320 nm long [23,24,28] [29]. Early studies demonstrated that mixtures of nonmuscle and sarcomeric myosins were capable of polymerizing into synthetic thick filaments

containing both myosins and that the thick filament length was inversely related to the percent of nonmuscle myosins [24,25]. The A-band widths of the fibers containing nmMyH IIB are 1.64±0.01 μm, the same as in somite-derived skeletal muscles and indicating that nmMyH IIB does not alter thick filament length in EOMs. The sarcomeric myosins translate actin filaments at much higher rates than nonmuscle or smooth muscle myosins [30]. Moreover, even small amounts of nonmuscle or smooth muscle myosins mixed with sarcomeric myosins significantly slow the rate of translation, indicating that the slower isoforms create drag [31]. nmMyH IIB has the highest duty cycle and is thus thought to produce the greatest tension of the nonmuscle myosins [32]. Thus, the A-band distribution of nmMyH IIB in these fibers may play a significant role in EOM function. nmMyH IIB consistently appears in a narrow band (220 nm in rat EOM, 230 nm in mouse EOM) within the center of the A-band, in the area normally containing the M-line in somite-derived skeletal muscles but known to be absent in EOMs. It is possible that nmMyH IIB in the center of the A-band prevents the formation of the M-line. However, it should be noted that the A-band distribution for nmMyH IIB is only found in 20% of the EOM global fibers, but the M-lines are missing in the whole muscle [9,10].

Sarcomeric myosins do not incorporate into the nonmuscle cytoskeleton when overexpressed in nonmuscle cells [33]. Instead, sarcomeric myosins are segregated in a chaperonin folding complex due to the lack of the muscle-specific chaperonin, Unc45b [34,35]. The myosin contained within these chaperonin complexes is filamentous in nature and is associated with nonmuscle myosin light chains [33,35]. We have been unable to detect nonmuscle myosin light chains in the sarcomeres containing nmMyH IIB. It remains to be seen what complement of light chains is associated with this mixed filament.

nmMyH IIB is essential for normal growth and development. The ablation of nmMyH IIB in mice is embryonic lethal due to hydrocephalus and severe cardiac defects [36]. Substitution of a GFP-tagged nmMyH IIA for the endogenous nmMyH IIB rescues from the hydrocephalic phenotype, but does not prevent cardiac defects and the mice die of dilated cardiomyopathy [37]. Tissue-specific deletion of nmMyH IIB induces cardiac and cerebral defects, underlying the importance of this nonmuscle myosin in these systems [38]. As in heart, somite-derived skeletal muscles have nmMyH IIB in the Z-lines [22,38]. The same is the case in EOM fibers, although the relatively higher content of nmMyH IIB in slow tonic fibers obscures this distribution and it is only evident when the imaging settings are modified to account for that (Figure 5B). The consequences of ablating nmMyH IIB in skeletal muscle exclusively remain unknown. However, nmMyH IIB has been postulated to play a role in myofibrillogenesis [39]. In both cardiac and somite-derived skeletal muscles, nmMyH IIB is associated with the pre-myofibrils of differentiating muscle cells [39]. In addition to nmMyH IIB, the pre-myofibrils contain sarcomeric α-actinin [39] and in cardiac muscle, nebulette [20,40]. With the addition of titin into the complex, the nonmuscle myosin is gradually replaced by sarcomeric myosin isoforms [39]. The EOMs are spared in muscular dystrophies associated with defects of the dystrophin-glycoprotein complex, an effect that may reflect constant regeneration within these muscles [41] [42-44]. The existence of nmMyH IIB-containing thick filaments in EOM fibers may be a direct result of this regenerative process.

Acknowledgments

The authors would like to thank Dr. Robert Adelstein for helpful suggestions on this work. We are also indebted to the members of the Center for Muscle Biology at UK for their insightful comments. This work was supported by grants from the National Eye Institute (NEI, part of NIH) to CLM (R21 EY018112) and FHA (R01 EY012998).

References

[1]. Evans DJ, Noden DM. Spatial relations between avian craniofacial neural crest and paraxial mesoderm cells. Dev Dyn 2006;235:1310–1325. [PubMed: 16395689]

[2]. Porter JD, Baker RS, Stava MW, Gaddie IB, Brueckner JK. Types and time course of the alterations induced in monkey blink movements by botulinum toxin. Exp Brain Res 1993;96:77–82. [PubMed: 8243585]

[3]. Sambasivan R, Gayraud-Morel B, Dumas G, Cimper C, Paisant S, Kelly RG, Tajbakhsh S. Distinct regulatory cascades govern extraocular and pharyngeal arch muscle progenitor cell fates. Dev Cell 2009;16:810–821. [PubMed: 19531352]

[4]. Mascarello F, Rowlerson AM. Myosin isoform transitions during development of extra-ocular and masticatory muscles in the fetal rat. Anat Embryol (Berl) 1992;185:143–153. [PubMed: 1531587]

[5]. Brueckner JK, Itkis O, Porter JD. Spatial and temporal patterns of myosin heavy chain expression in developing rat extraocular muscle. J Muscle Res Cell Motil 1996;17:297–312. [PubMed: 8814550]

[6]. Pedrosa-Domellof F, Holmgren Y, Lucas CA, Hoh JF, Thornell LE. Human extraocular muscles: unique pattern of myosin heavy chain expression during myotube formation. Invest Ophthalmol Vis Sci 2000;41:1608–1616. [PubMed: 10845576]

[7]. Anderson JE, Kao L, Bressler BH, Gruenstein E. Analysis of dystrophin in fast- and slow-twitch skeletal muscles from mdx and dy2J mice at different ages. Muscle & Nerve 1990;13:6–11. [PubMed: 2183046]

[8]. McMullen CA, Hayess K, Andrade FH. Fatigue resistance of rat extraocular muscles does not depend on creatine kinase activity. BMC Physiol 2005;5:12. [PubMed: 16107216]

[9]. Mayr R. Structure and distribution of fibre types in the external eye muscles of the rat. Tissue Cell 1971;3:433–462. [PubMed: 18631565]

[10]. Andrade FH, Merriam AP, Guo W, Cheng G, McMullen CA, Hayess K, van der ven PF, Porter JD. Paradoxical absence of M lines and downregulation of creatine kinase in mouse extraocular muscle. J Appl Physiol 2003;95:692–699. [PubMed: 12716871]

[11]. Porter JD, Merriam AP, Gong B, Kasturi S, Zhou X, Hauser KF, Andrade FH, Cheng G. Postnatal suppression of myomesin, muscle creatine kinase and the M-line in rat extraocular muscle. J Exp Biol 2003;206:3101–3112. [PubMed: 12878677]

[12]. Grove BK, Cerny L, Perriard JC, Eppenberger HM. Myomesin and M-protein: expression of two M-band proteins in pectoral muscle and heart during development. J Cell Biol 1985;101:1413–1421. [PubMed: 4044641]

[13]. Agarkova I, Auerbach D, Ehler E, Perriard JC. A novel marker for vertebrate embryonic heart, the EH-myomesin isoform. J Biol Chem 2000;275:10256–10264. [PubMed: 10744711]

[14]. Khanna S, Cheng G, Gong B, Mustari MJ, Porter JD. Genome-wide transcriptional profiles are consistent with functional specialization of the extraocular muscle layers. Invest Ophthalmol Vis Sci 2004;45:3055–3066. [PubMed: 15326121]

[15]. Cheng G, Merriam AP, Gong B, Leahy P, Khanna S, Porter JD. Conserved and muscle-group-specific gene expression patterns shape postnatal development of the novel extraocular muscle phenotype. Physiol Genomics 2004;18:184–195. [PubMed: 15138310]

[16]. Ravenscroft G, Colley SM, Walker KR, Clement S, Bringans S, Lipscombe R, Fabian VA, Laing NG, Nowak KJ. Expression of cardiac alpha-actin spares extraocular muscles in skeletal muscle alpha-actin diseases--quantification of striated alpha-actins by MRM-mass spectrometry. Neuromuscul Disord 2008;18:953–958. [PubMed: 18952430]

[17]. Moncman CL, Andrade FH. Nebulin isoforms of extraocular muscle. Cell Tissue Res 2007;327:415–420. [PubMed: 17053899]

[18]. Li B, Zhuang L, Trueb B. Zyxin interacts with the SH3 domains of the cytoskeletal proteins LIM-nebulette and Lasp-1. J Biol Chem 2004;279:20401–20410. [PubMed: 15004028]

[19]. Gauthier GF. Differential distribution of myosin isoforms among the myofibrils of individual developing muscle fibers. J. Cell Biol 1990;110:693–701. [PubMed: 2307704]

[20]. Moncman CL, Wang K. Nebulette: a 107 kD nebulin-like protein in cardiac muscle. Cell Motility & the Cytoskeleton 1995;32:205–225. [PubMed: 8581976]

[21]. Spencer RF, Porter JD. Biological organization of the extraocular muscles. Prog Brain Res 2006;151:43–80. [PubMed: 16221585]

[22]. Takeda K, Yu ZX, Qian S, Chin TK, Adelstein RS, Ferrans VJ. Nonmuscle myosin II localizes to the Z-lines and intercalated discs of cardiac muscle and to the Z-lines of skeletal muscle. Cell Motil Cytoskeleton 2000;46:59–68. [PubMed: 10842333]

[23]. Huxley HE. Electron Microscope Studies on the Structure of Natural and Synthetic Protein Filaments from Striated Muscle. J Mol Biol 1963;7:281–308.

[24]. Pollard TD. Electron microscopy of synthetic myosin filaments. Evidence for cross-bridge. Flexibility and copolymer formation. J Cell Biol 1975;67:93–104. [PubMed: 1236853]

[25]. Wachsberger PR, Pepe FA. Interaction between vertebrate skeletal and uterine muscle myosins and light meromyosins. J Cell Biol 1980;85:33–41. [PubMed: 6988442]

[26]. Cynader M. Interocular alignment following visual deprivation in the cat. Invest Ophthalmol Vis Sci 1979;18:726–741. [PubMed: 447471]

[27]. Spencer RF, Porter JD. Structural organization of the extraocular muscles. Rev Oculomot Res 1988;2:33–79. [PubMed: 3153651]

[28]. Niederman R, Pollard TD. Human platelet myosin. II. In vitro assembly and structure of myosin filaments. J Cell Biol 1975;67:72–92. [PubMed: 240861]

[29]. Svitkina TM, Verkhovsky AB, Borisy GG. Improved procedures for electron microscopic visualization of the cytoskeleton of cultured cells. Journal of Structural Biology 1995;115:290–303. [PubMed: 8573471]

[30]. Vicente-Manzanares M, Ma X, Adelstein RS, Horwitz AR. Non-muscle myosin II takes centre stage in cell adhesion and migration. Nat Rev Mol Cell Biol 2009;10:778–790. [PubMed: 19851336]

[31]. Cuda G, Pate E, Cooke R, Sellers JR. In vitro actin filament sliding velocities produced by mixtures of different types of myosin. Biophys J 1997;72:1767–1779. [PubMed: 9083681]

[32]. Wang F, Kovacs M, Hu A, Limouze J, Harvey EV, Sellers JR. Kinetic mechanism of non-muscle myosin IIB: functional adaptations for tension generation and maintenance. J Biol Chem 2003;278:27439–27448. [PubMed: 12704189]

[33]. Moncman CL, Rindt H, Robbins J, Winkelmann DA. Segregated assembly of muscle myosin expressed in nonmuscle cells. Mol. Biol. Cell 1993;4:1051–1067. [PubMed: 8298191]

[34]. Srikakulam R, Winkelmann DA. Myosin II folding is mediated by a molecular chaperonin. J Biol Chem 1999;274:27265–27273. [PubMed: 10480946]

[35]. Srikakulam R, Winkelmann DA. Chaperone-mediated folding and assembly of myosin in striated muscle. J Cell Sci 2004;117:641–652. [PubMed: 14709723]

[36]. Tullio AN, Accili D, Ferrans VJ, Yu ZX, Takeda K, Grinberg A, Westphal H, Preston YA, Adelstein RS. Nonmuscle myosin II-B is required for normal development of the mouse heart. Proc Natl Acad Sci U S A 1997;94:12407–12412. [PubMed: 9356462]

[37]. Bao J, Ma X, Liu C, Adelstein RS. Replacement of nonmuscle myosin II-B with II-A rescues brain but not cardiac defects in mice. J Biol Chem 2007;282:22102–22111. [PubMed: 17519229]

[38]. Ma X, Takeda K, Singh A, Yu ZX, Zerfas P, Blount A, Liu C, Towbin JA, Schneider MD, Adelstein RS, Wei Q. Conditional ablation of nonmuscle myosin II-B delineates heart defects in adult mice. Circ Res 2009;105:1102–1109. [PubMed: 19815823]

[39]. Rhee D, Sanger JM, Sanger JW. The premyofibril: evidence for its role in myofibrillogenesis. Cell Motility & the Cytoskeleton 1994;28:1–24. [PubMed: 8044846]

[40]. Esham M, Bryan K, Milnes J, Holmes WB, Moncman CL. Expression of nebulette during early cardiac development. Cell Motil Cytoskeleton 2007;64:258–273. [PubMed: 17238151]

[41]. Porter JD, Rafael JA, Ragusa RJ, Brueckner JK, Trickett JI, Davies KE. The sparing of extraocular muscle in dystrophinopathy is lost in mice lacking utrophin and dystrophin. J Cell Sci 1998;111(Pt 13):1801–1811. [PubMed: 9625743]

[42]. McLoon LK, Wirtschafter J. Activated satellite cells are present in uninjured extraocular muscles of mature mice. Trans Am Ophthalmol Soc 2002;100:119–123. discussion 123-114. [PubMed: 12545684]

[43]. McLoon LK, Rowe J, Wirtschafter J, McCormick KM. Continuous myofiber remodeling in uninjured extraocular myofibers: myonuclear turnover and evidence for apoptosis. Muscle Nerve 2004;29:707–715. [PubMed: 15116375]

[44]. Wirtschafter JD, Ferrington DA, McLoon LK. Continuous remodeling of adult extraocular muscles as an explanation for selective craniofacial vulnerability in oculopharyngeal muscular dystrophy. J Neuroophthalmol 2004;24:62–67. [PubMed: 15206442]

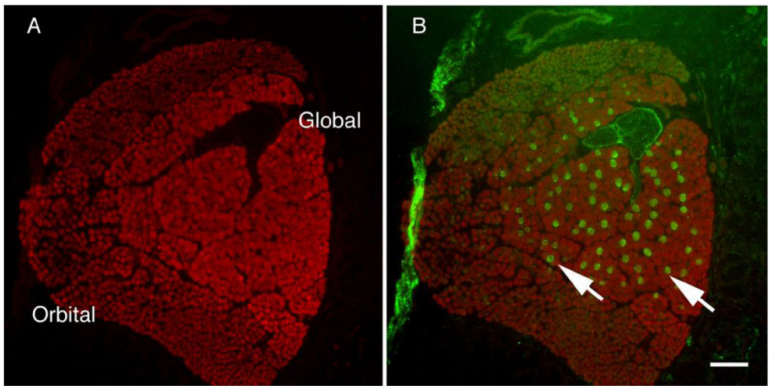

Figure 1.
Low magnification of rat rectus muscle. An entire rat rectus muscle was stained for sarcomeric α-actinin (A) or α-actinin (red in B) and counter-stained for nmMyH IIB (green in B). The α-actinin staining in panel A clearly shows the layers of the EOMs and they are labeled as such. The fibers strongly positive for nmMyH IIB (green in B) are localized to the global layer only (arrows). Scale bar = 100 μm.

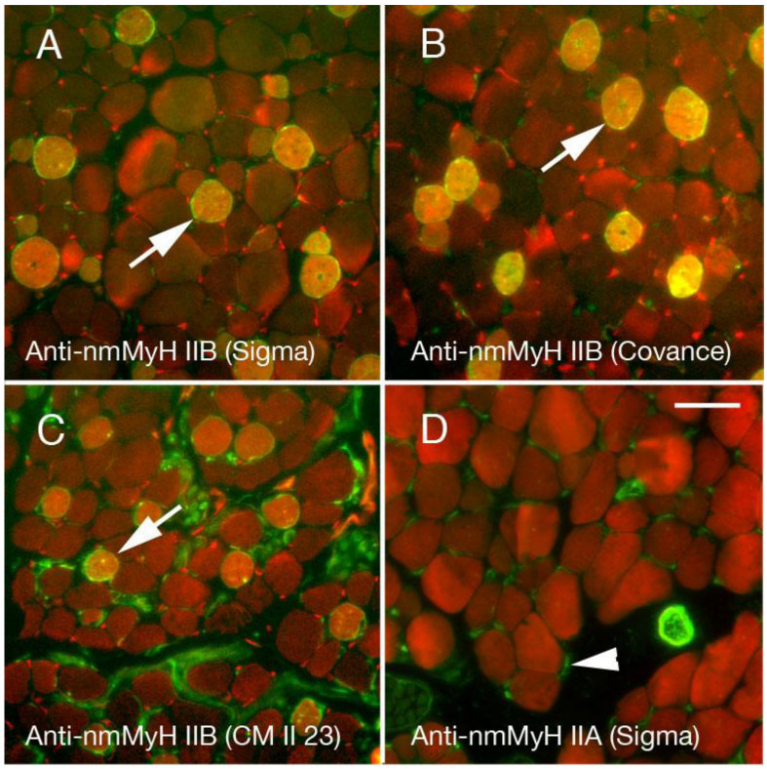

Figure 2.

Adult rat orbits stained for the distribution of nmMyH IIB (green in A-C) using three different antibodies against this protein or IIA (green in D) vs. actin (red in all fields). The polyclonal antibodies are raised against the non-helical tailpiece of myosin and highly label a subset of fibers in the global layers of EOMs (A, B). The monoclonal antibody CM23 II detects nmMyH IIB positive fibers, but labels the neurons better (C). Arrows mark examples of the high level of labeling in A-C. The anti-nmMyH IIA stains satellite cells, neurons, and blood vessels, but nothing within the muscle fibers. Scale bar =10 μm.

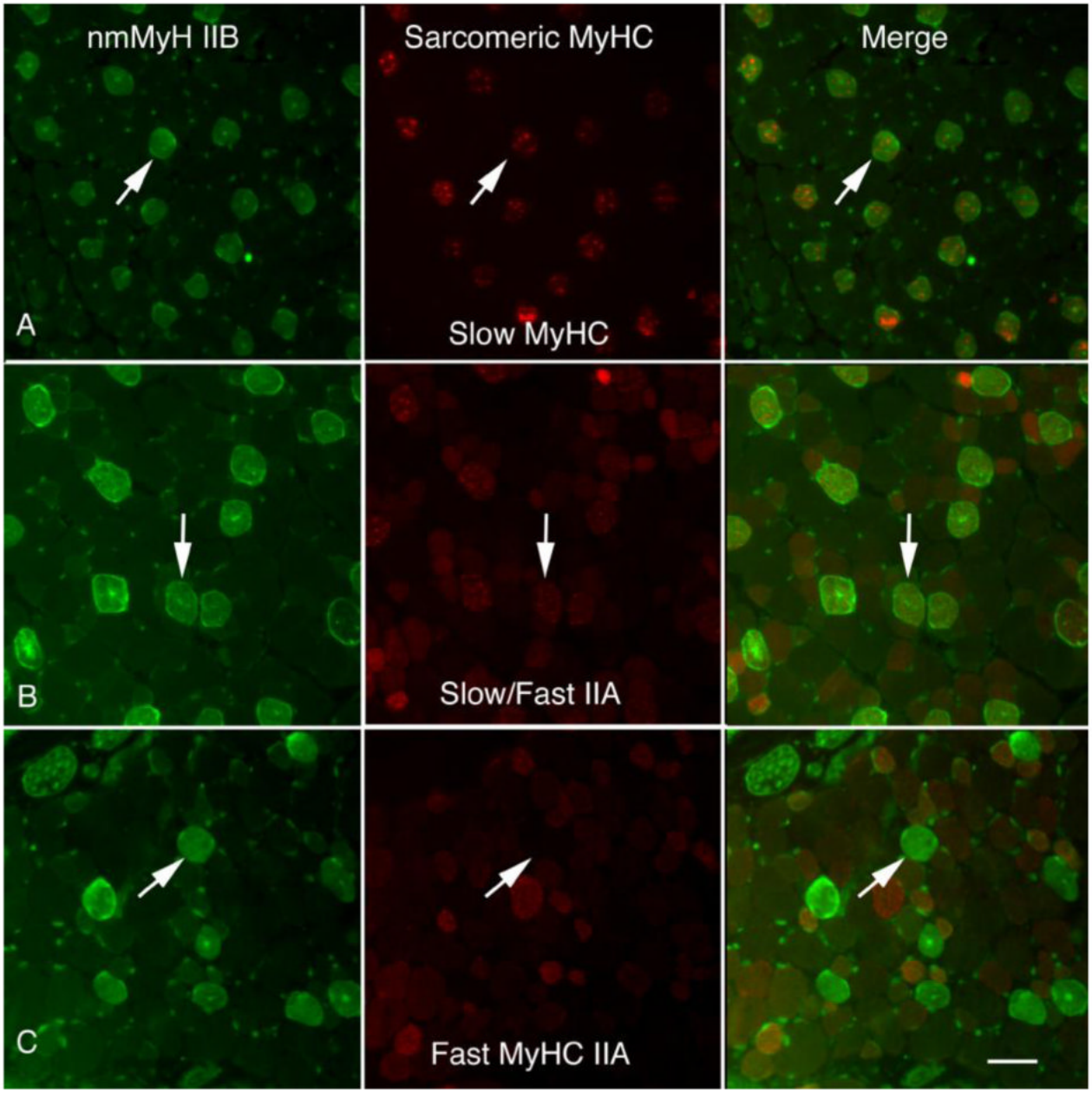

Figure 3.

Comparison of nmMyH IIB with sarcomeric myosins. Cross-sections of rat orbits were stained with anti-nmMyH IIB antibodies and counterstained with monoclonal antibodies A4.951 (adult slow in A), N2.251 (slow/fast 2A in B) or 2F7 (fast 2A in C). The fibers that exhibit strong staining for nmMyH IIB also exhibit strong staining for the anti-slow sarcomeric MyHC (note arrows in A and B). Additional fibers in B stain with N2.261 are presumably due to the cross reactivity of this antibody with the MyHC fast 2A isoform. The intrafiber staining of nmMyH IIB did not coincide with fibers expressing fast sarcomeric isoforms. Arrows indicate the position of the same fibers in all three panels. Scale bar =10 μm.

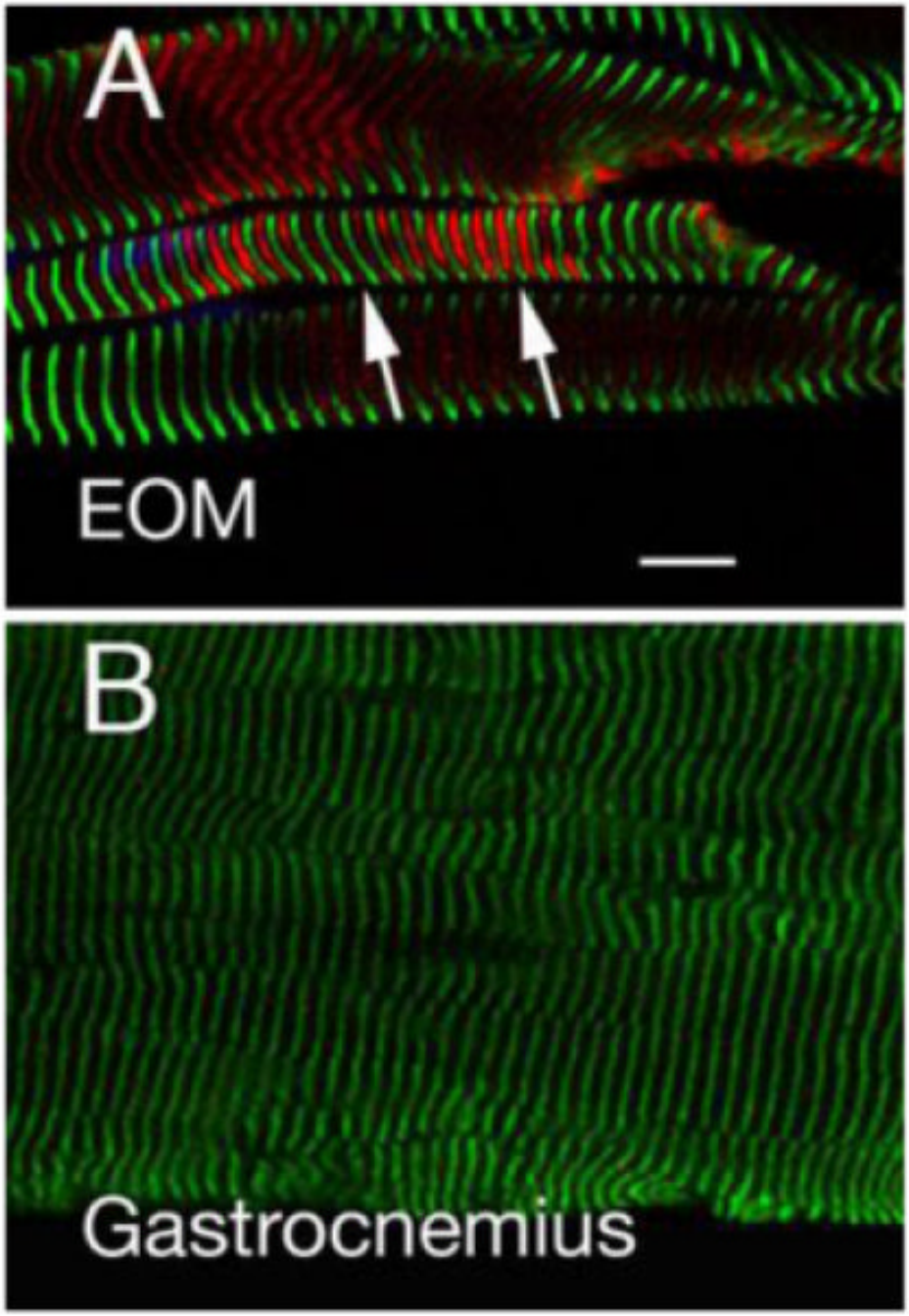

Figure 4.
EOM and gastrocnemius muscle sections labeled with antibodies to α-actinin (green, marks Z lines) or nmMyH IIB (red). The gain and offset for the EOM were set at 654 and −1.8 and the image for gastrocnemius was collected at the same settings. The images show that nmMyH IIB is present between the Z lines in EOM sarcomeres (note arrows in A). On the other hand, nmMyH IIB is not visible in gastrocnemius (B). Scale bar = 10 μm.

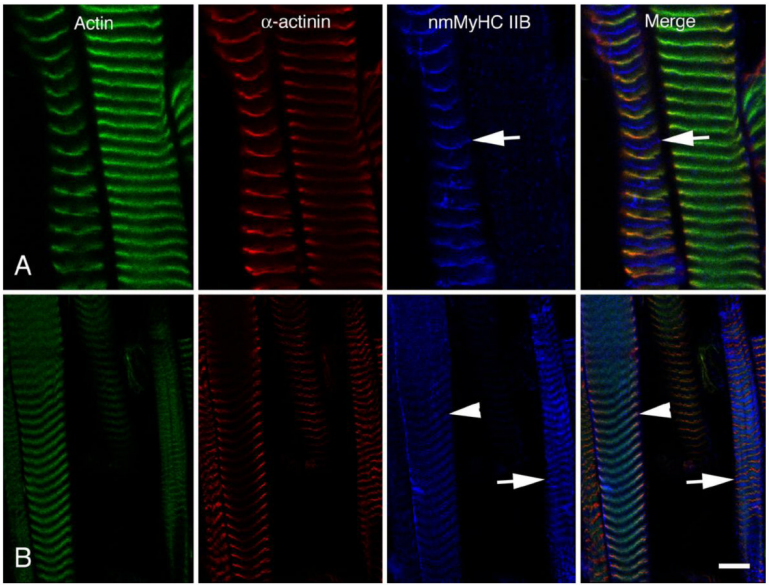

Figure 5.

Longitudinal sections of rat EOM that have been relaxed, chemically skinned and stretched. EOMs were dissected out and placed in relaxing buffer for several hours prior to flash freezing. The upper and lower panels compare the distribution of actin (green), α-actinin (red) and nmMyH IIB (pseudo blue). The gain and offset were set for optimal exposure of the nmMyH IIB in A; whereas in B the gain and offset were set to bring up the exposure of the much weaker Z-line distribution of the nmMyH IIB. The arrows indicate the A-band distribution of nmMyH IIB in both A and B). The arrowheads indicate the labeling on nmMyH IIB at the Z-line. Under these conditions the A-band distribution appears much broader in B due to saturation of the signal. Scale bar = 5 μm in upper panels and 10 μm in lower.

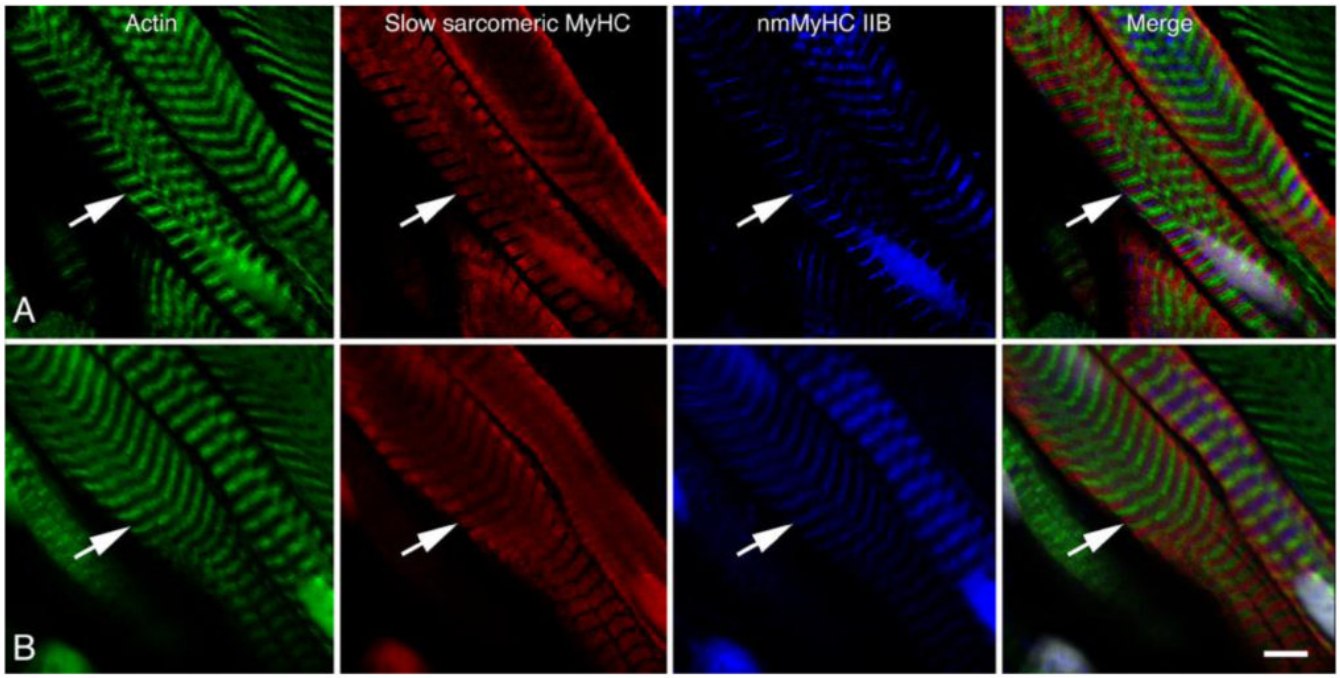

Figure 6.

Comparison of the distribution of nmMyH IIB (pseudo blue) with the distribution of slow sarcomeric MyHC (red), actin (green) and nuclei (grey). Muscle in panel A was relaxed and flash frozen prior to sectioning, while muscle in panel B was fixed in 4% formaldehyde prior to processing. In both cases, the antibodies to nmMyH IIB label a distinct strip in the middle of the A-bands containing slow sarcomeric myosins (note arrows in both panels). The observed A-band distribution of nmMyH IIB is independent of fixation conditions. Scale bar = 5 μm.

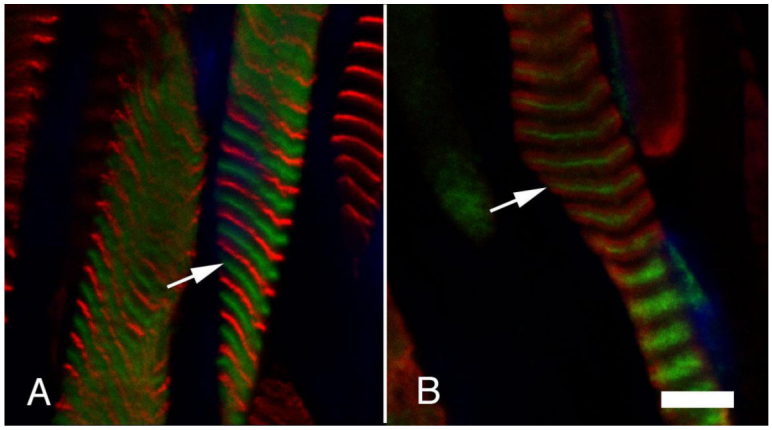

Figure 7.

Adult mouse EOMs were dissected out and stretched in relaxing buffer for four hours prior to snap freezing. Cryostat sections were stained with antibodies to nmMyH IIB (green in A and B) and antibodies to α-actinin (A) or slow sarcomeric myosin (B) (red). Nuclei are shown in blue. The A-band distribution of nmMyH IIB is also evident in mouse EOMs. Scale bar = 5 μm.